Fouling of Steam Generator Tubes in Nuclear Power Plants : Investigation on the Preventive Effect of Polyacrylic Acid on Iron Oxides Deposition

Marion Roy, Ricardo d'Angelo, Dominique You, Sophie Delaunay, Thierry Pauporte, Jean-Luc Bretelle

Fouling of Steam Generator Tubes in Nuclear Power Plants: Investigation on the Preventive Effect of Polyacrylic Acid on Iron Oxides Deposition
-18-

Marion Roy[1], Ricardo D'Angelo[2,3], Dominique You[1], Sophie Delaunay[2], Thierry Pauporté[3], Jean-Luc Bretelle[4]

[1] Den-Service d'Etude du Comportement des Radionucléides (SECR), CEA, Université Paris-Saclay, F-91191, Gif-sur-Yvette, France

[2] EDF R&D/Chemistry and Corrosion Group, Avenue des Renardières, 77818 Moret-sur-Loing Cedex, France

[3] Chimie ParisTech, PSL Research University, CNRS, Institut de Recherche de Chimie Paris (IRCP), 11 rue P. et M. Curie, F-75005 Paris, France.

[4] EDF/Power Generation Division, 1 Place Pleyel, 93200 Saint Denis, France

ABSTRACT

In order to reduce and prevent the fouling and blockage of Steam Generators (SGs), one of the approaches of nuclear operators consists in injecting PolyAcrylic Acid (PAA) as a dispersing agent. The goal of this injection is to prevent corrosion products deposition on the surface of SG tubes and to facilitate their evacuation through the SG blowdown circuit.

The aim of this study was to evaluate the preventive nature of PAA on the fouling deposits (mainly composed of iron oxides) in SGs and to determine the action mechanism(s) of PAA on iron oxides.
The investigation of the effect of PAA on magnetite suspensions and on the formation of deposit layers onto (pre-oxidized) Inconel 690TT tubes was conducted. This was performed in a dedicated biphasic loop reproducing the physico-chemical conditions of pressurized water reactor SGs. The results showed an increased iron concentration at the loop exit with the injection of PAA. Characterizations of the samples indicated the apparent diminution of oxide layer thickness and a change in oxide phase from magnetite to hematite at the liquid-steam interface region in the reactor. The study of these effects led us to the critical discussion of the hypotheses which can explain the underlying action mechanisms of PAA.

Moreover, the SG fouling, including an injection of PAA, has been modelled and showed an increase of iron quantity at SG blowdown. The proposed model was based on the physico-chemistry mechanisms occurring in SG. The chemical code PhreeqCEA-3.2 version[1] dedicated to reactors application was successfully used.

INTRODUCTION

The transport and deposition of corrosion products, composed primarily of magnetite (Fe_3O_4), in Steam Generators (SGs) promotes the fouling of SGs tubes and the blockage of the broached tube support plates of SGs units. These corrosion products are generated by the corrosion of components of the feedwater line

---

[1] CEA chemical code dedicated to reactors application, developed from USGS software PHREEQC

of the Pressurized Water Reactor (PWR). The fouling and the blockage of the SGs decrease the thermal efficiency and increase the maintenance costs. In this respect, it is critical that the deposition of these corrosion products in the SGs be limited.

In order to limit the blockage and the fouling in SGs, nuclear operators currently utilize chemical conditioning, chemical cleaning techniques (STUZMANN et al., 2015) and mechanical techniques. Another way is the use of the online injection of a dispersant, PolyAcrylic Acid (PAA) into the SGs during operation.

The study of the impact of PAA on magnetite particles in suspension and on the formation of oxide deposits on SGs materials has been of interest for its application into the nuclear park. The interactions occurring between PAA and the iron could lead to a reduction in the deposit formation kinetics, which would inhibit the formation of deposits. Such an application would strongly be beneficial for the operation of the SGs.

Dispersant injection in nuclear power plants has been investigated for long-term use in the USA (EPRI, 2012). Two types of application methods are in use at Nuclear Power Plants (NPPs): the online long-term use and the offline applications which include SG wet layup and startup long-path recirculation. Online applications have also been performed in France (Golfech 2) (low quantity of PAA during the cycle) and in Belgium (Doel 3) (LAIRE et al., 2014) (high quantity of PAA at the end of the cycle).

The aim of this study was to evaluate the preventive nature of PAA on the fouling deposits (mainly composed of iron oxides) in SGs and to determine the action mechanism(s) of PAA on iron oxides. The modelling of SGs fouling and the preventive PAA effect on iron was also realized.

EXPERIMENT DESCRIPTION

Two experiments were carried out using magnetite powder and Inconel 690TT tubes:

- one blank test without PAA (Test 0) was performed in order to determine the effect of the secondary conditioning on the tube and on the dissolved iron content in solution. It will be a reference for further comparison;

- one test with 0.1 mg.kg^{-1} of PAA (Test 0.1) to evaluate the PAA effect on the quantity of solubilized iron but also on the iron oxide deposition on the tube. The value of the tested concentration was chosen to be high enough to see an effect after a trial of 60 days duration and in the area of interest of a PWR operator.

To evaluate the effect of PAA on the magnetite particles in suspension and its effect on the formation of oxide deposits, studies were performed in physico-chemical conditions representative of the SGs. Tests were performed by inserting a SG tube made of Inconel alloy 690TT, measuring one meter in length in the IRIS loop shown in Figure 1. This loop was designed to reproduce the operational conditions of the secondary side two phase flow section of the SG of the PWR plants. A simplified scheme of the system is shown in Figure 1. The solution circulated around the exterior surface of the tube which, was heated from inside to a temperature of 283 °C thanks to a steam primary circuit (not represented in Figure 1) heated to 302 °C.
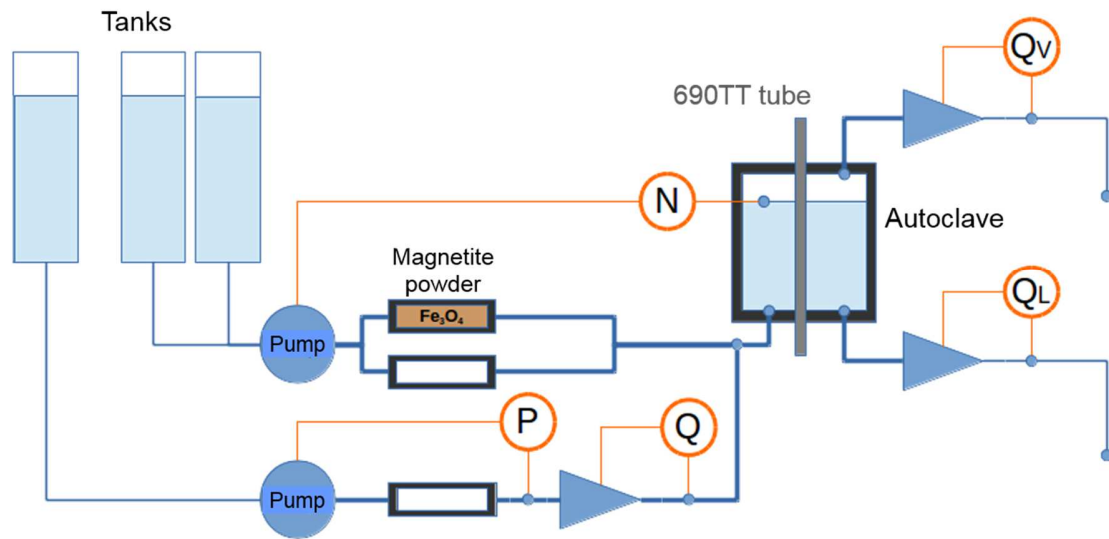
Figure 1. Simplified scheme of the setup named IRIS (for Research Instrumentation for the Investigation of Speciation in aqueous media at high temperature) ROY, BLANCHARD, MERTENS, & YOU (2014).
(P: pressure, N: level of the liquid/steam interface, Q: mass flow of the conditioning at the input,
Q_V: mass flow of steam at the output, Q_L: mass flow of liquid at the output)

The tests were conducted in two phases: the tubes were first subjected to one month of pre-oxidation at 283 °C and then to one month with injection of magnetite particles (purity level of 97 %) at 283 °C. The pre-oxidation consisted in injecting the conditioned water into the heated autoclave directly whereas the following month, the conditioned water passed through the magnetite powder containing cell (80 g) prior to enter into the autoclave.

The test conditions and parameters used in the IRIS loop for the preventive study tests are summarized in Table 1. To obtain a reducing media, the solutions are deaerated at least 4 hours under vacuum and the conditioned solution was continuously bubbled in the tanks using Ar-5 % H_2 gas.

The expected iron concentration in SG feedwater is about 2×10^{-6} g.kg^{-1} (EPRI, 2002). Because of the important solution flow in the magnetite containing cell, the equilibrium cannot be reached in this cell. To enable iron deposition on the Inconel tube, the iron content has to be higher than the solubility limit of iron at 280 °C ($S_{Fe}(280\ °C) = 4\times10^{-8}$ mol.kg^{-1} $\approx 2\times10^{-6}$ g.kg^{-1}). As a consequence, the cell was heated at 140 °C in order to reach an equilibrium iron content equal to 3×10^{-7} mol.kg^{-1} *i.e.* 17×10^{-6} g.kg^{-1}.

Table 1. Parameters and physico-chemical conditions utilized for IRIS experiments

	T	P	pH	t_R	Duration	[PAA]	[Morpholine]	[NH$_4$OH][1]
Units	°C	10^6 Pa	à 25 °C	h	h	mg.kg^{-1}	mg.kg^{-1}	mg.kg^{-1}
Test 0	283 ± 2	6.7 ± 0.2	9.6 ± 0.5	28	1500	0	5.5	≈ 1.5
Test 0.1	283 ± 2	6.7 ± 0.2	9.6 ± 0.5	28	1500	0.1	5.5	≈ 1.5

[1] NH$_4$OH is used to adjust the pH to 9.6

Upon completion of each test, the SG tube was removed from the autoclave. Then it was photographed, sectioned (Figure 2) and cut into pieces thanks to the position in the reactor. To evaluate the effect of PAA on the formation of oxide deposits, characterization of these tube sections was realized. Only the results of the autoclave zone (see Figure 2) are presented in the next section.
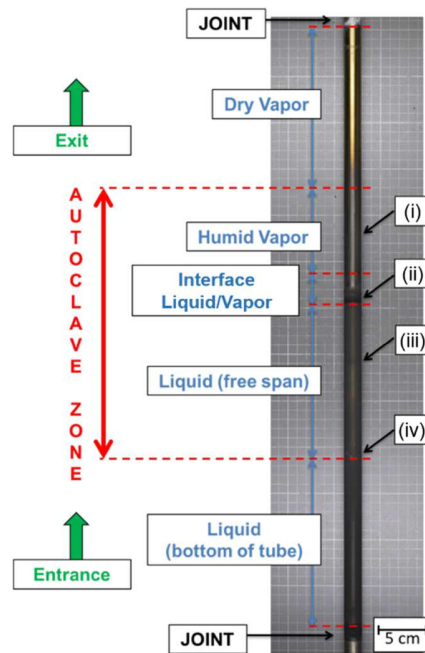

Figure 2. Sections of IRIS tube analysed by SEM and XRD

RESULTS and DISCUSSION

Preventive effect of PAA

This section presents the results pertaining to the effect of PAA on magnetite particles in solution and the effect of PAA on the formation of deposits.

Atomic Adsorption Spectroscopy (AAS) measurements at the entrance and exit (both liquid and vapour) of the IRIS loop were performed to follow the iron concentration evolution with the addition of PAA (see Table 2). The results seem to show a PAA effect, employed in a preventive way on iron for a PAA concentration 0.1 mg.kg^{-1}. The dissolved iron content is increased by a 3.3 factor on average at the liquid exit in the presence of PAA and can be up to 6 times higher than the iron content measured without PAA. It was also observed a decrease in the stabilization time of the iron concentration. The stabilization of the iron content occurred after 300 h to 120 h without and with the addition of PAA, respectively. This PAA effect on the magnetite particles in solution was demonstrated previously in the works by (REILLER et al., 2011; ROY, MANSOUR, & YOU, 2014).

Table 2. AAS measurements of iron concentration values at the entrance and exits
of the IRIS loop after introduction of Fe_3O_4

	Test 0	Test 0.1
	[Fe] ($\mu g.kg^{-1}$)	[Fe] ($\mu g.kg^{-1}$)
Entry	3 ± 3	3 ± 3
Liquid exit	4 ± 1	13 ± 7
Vapour exit	2 ± 1	3 ± 1

Initial indications of the effect of PAA on the formation of oxide deposits are shown by the visual aspect of the tube after the tests without PAA and with PAA (Figure 3). The test without PAA gave rise to a black deposit in the form of a gradient going from lightest in the humid steam phase to darkest in the liquid phase. However, after testing with PAA another gradient, this time composed of several phases, was observed (Figure 3 (iii)) including a red one (in (ii) section) which is supposed to be hematite.
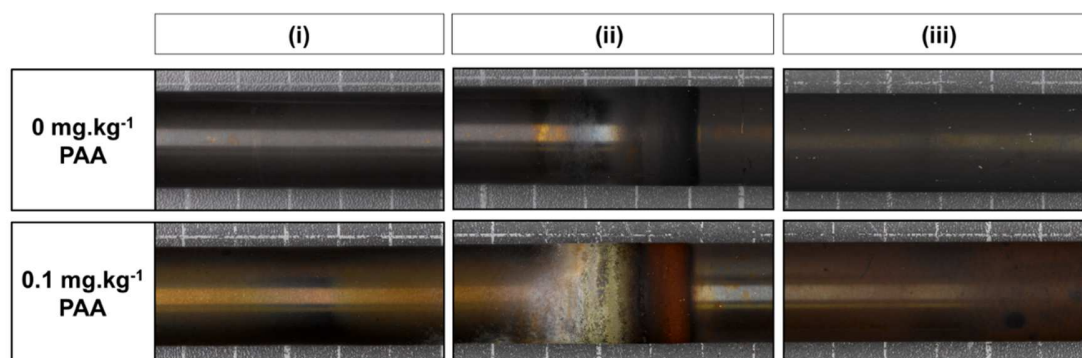

Figure 3. Photograph of the (i) humid vapour section, (ii) liquid/vapour interface section and (iii) liquid section of the IRIS tube after testing at 0 and 0.1 mg.kg^{-1} PAA

In the liquid free-span phase (Figure 2 (iii)) there was an observed apparent decrease in the oxide deposit formed on the surface of the tube in the presence of PAA. This decrease was confirmed by XRD analysis performed on the same tube section. Indeed, the results showed a decrease of magnetite pattern signal when 0.1 mg.kg^{-1} PAA was injected. Moreover, the decrease was notable thanks to the reduction of the amount of agglomerated or grouped particles, as-shown in Figure 5.
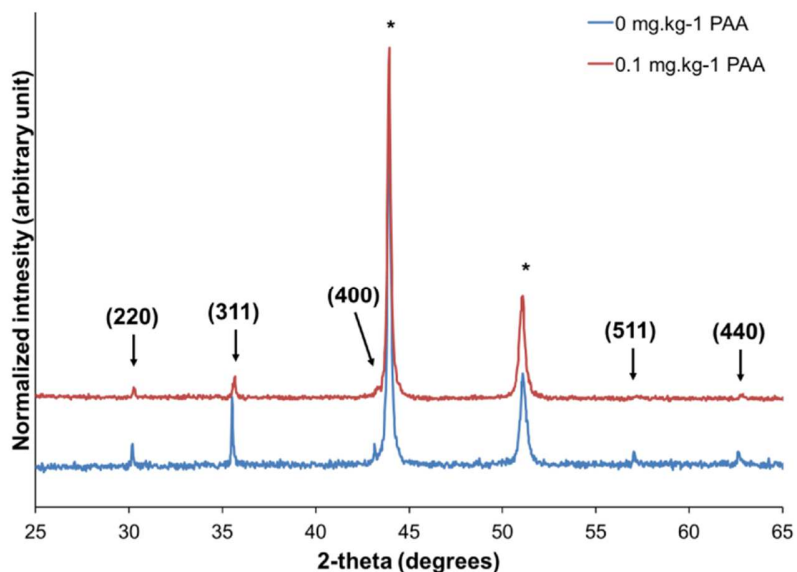
Figure 4. X-ray Diffraction pattern for the IRIS tube at the liquid free-span section (Figure 2 (iii)), deposited in the presence and absence of PAA. The * indicates peaks corresponding to Inconel 690TT, (CuKα radiation = 1.5418 Å)
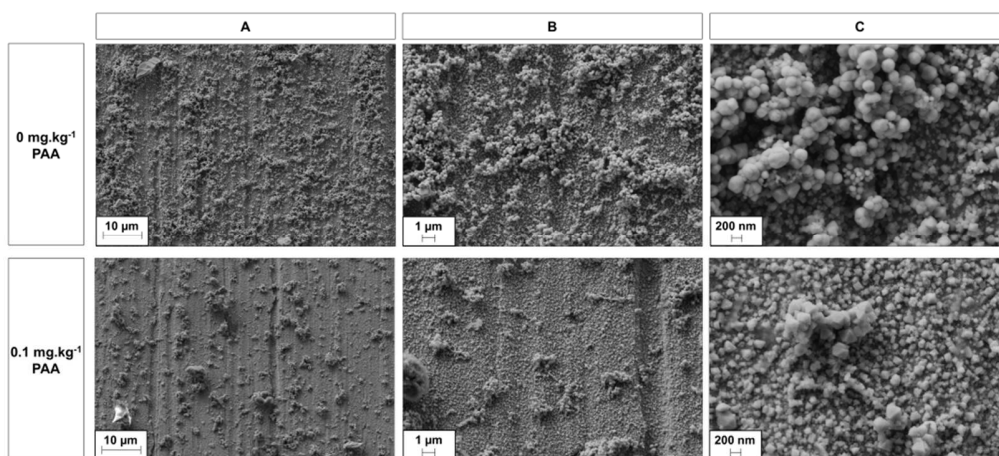

Figure 5. SEM-secondary electron images of the tube surface in the liquid free span after the reference test and the test containing 0.1 mg.kg^{-1} PAA

The particles deposited in both cases were in the form of octahedron from less than 200 nm to at least 1 μm in diameter for both tests. However, for the test with PAA there was a more numerous amount of large octahedra. This could be an indication of the effect of PAA on the germination and growth kinetics on iron oxides.

Hematite formation on the tube surface

The presence of PAA in the circuit seems to lead to the formation of hematite (α-Fe_2O_3) on the tube surface of Inconel 690TT. A red phase is distinguished on the SG tube at the liquid/vapour interface (Figure 3 (ii))

when PAA is injected (Test 0.1). XRD analyses of this section (Figure 1) after PAA injection, indicated the presence of hematite patterns (shown in green), showing that PAA had an effect on the particle crystallization.
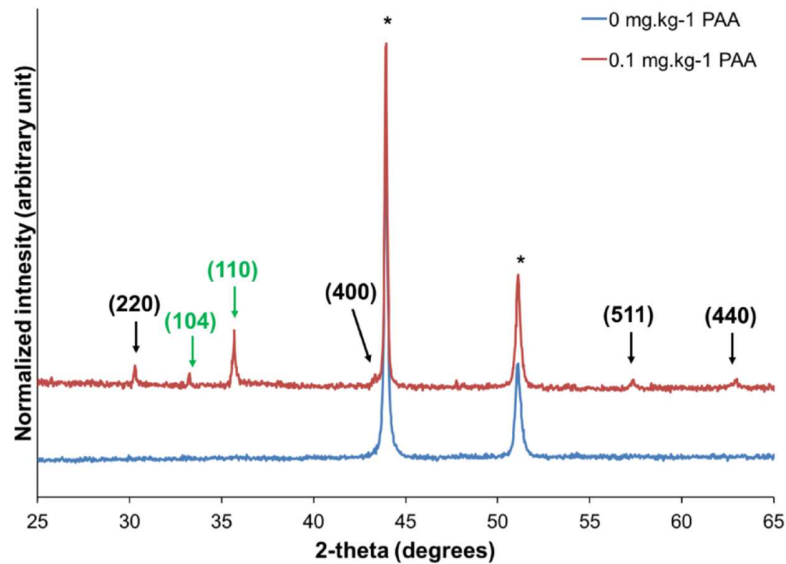

Figure 6. X-ray diffraction pattern for the IRIS tube at the liquid-vapour interface section, deposited in the presence and absence of PAA, where the peaks in green are assigned to hematite contribution to the XRD pattern. The * indicates peaks corresponding to Inconel 690TT, (CuKα radiation = 1.5418 Å)

SEM observations were also made on the red zone of the tube (Figure 3 (ii)). It showed the presence of crystal platelets (Figure 7 (a)) with a shape close to that reported by SAPIESZKO & MATIJEVIĆ (1980) for hematite powders prepared by hydrothermal growth .

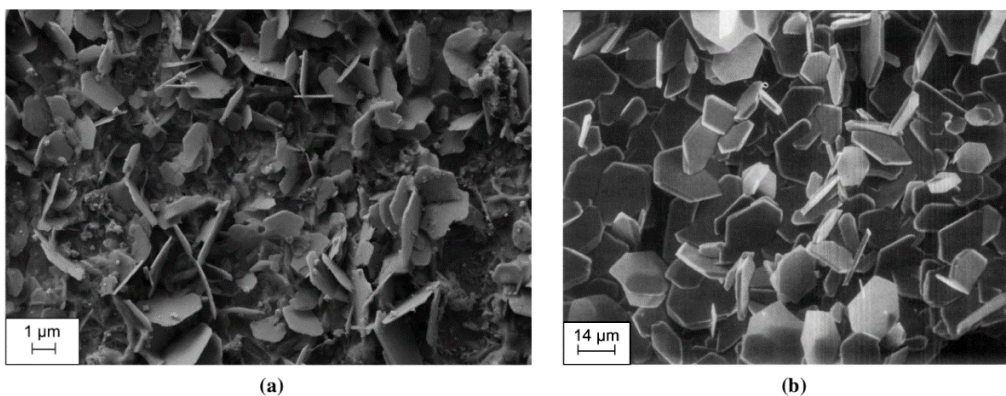Figure 7. SEM-secondary electron images of (a) liquid/vapor interface section after testing at 0.1 mg.kg^{-1} PAA in IRIS and (b) pure hematite produced by hydrothermal growth in the work by SAPIESZKO & MATIJEVIĆ (1980)

According to the Pourbaix diagram of iron-water at 25 °C (POURBAIX, 1963), the stable phase of iron is magnetite at pH 9.6 in reducing conditions. The same stable phase is found at higher temperature for the

same pH (ANGWIN, 1986). As a consequence, from a thermodynamic point of view hematite should not form in the SG.

The first hypothesis links the formation of hematite to an interaction of PAA with the iron (II) in water (Equation 1). The iron (II) was complexed by PAA shifting the equilibrium towards the right and thus iron (III) in solution precipitated as hematite which could have been deposited on the surface.

$$Fe^{II}Fe_2^{III}O_4 + 2H^+ \leftrightarrow Fe^{2+} + \alpha - Fe_2O_3 + H_2O \tag{1}$$
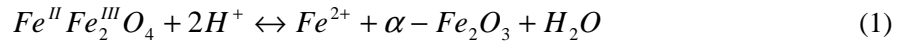
This balanced chemical equation (Equation 1) can be divided in the following steps. First, magnetite dissolution at the oxide/solution interface, leads to the formation of iron (II) and iron (III) according to Equation 2:

$$Fe^{II}Fe_2^{III}O_4 + 8H^+ \leftrightarrow Fe^{II} + 2Fe^{III} + 4H_2O \tag{2}$$
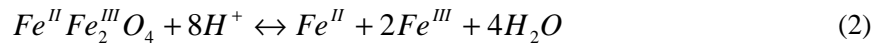
In presence of dihydrogen, iron (III) is reduced in iron (II). The equilibrium is given Equation 3.

$$2Fe^{III} + H_2 \leftrightarrow 2Fe^{II} + 2H^+ \tag{3}$$

Then, the sum of Equations 2 and 3 leads to the equilibrium reaction of magnetite dissolution which occurs in a reduce media (Equation 4).

$$Fe^{II}Fe_2^{III}O_4 + 6H^+ + H_2 \leftrightarrow 3Fe^{II} + 4H_2O \tag{4}$$
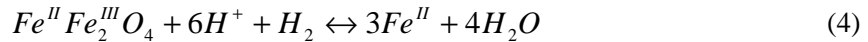
For the test with 0.1 mg.kg^{-1} of PAA, the complexation of iron (II) by PAA shifts the equilibrium (2) to the right. Then, the formation of iron (III) is increased. Since, hematite is formed from iron (III) (see Equation 5), this complexation favours the formation of hematite rather than magnetite.

$$2Fe^{III} + 3H_2O \leftrightarrow \alpha - Fe_2O_3 + 6H^+ \tag{5}$$
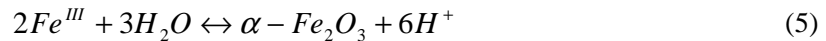
Moreover, the reduction of iron (III) into iron (II) (Equation 3) consumes the dihydrogen in the solution close to the interface oxide/solution. As a consequence, the redox potential increases locally, which enhances the formation of hematite on the oxide surface. The evaporation at the liquid/vapour interface leads to an overconcentration of PAA that could explain this phenomenon.

The redox potential can also be modified at the liquid/steam interface because of the thermal degradation products of PAA. The main degradation products, formate and acetate (ROY, MANSOUR, et al., 2014), could create localized areas of oxidation, which in turn oxidize the magnetite forming hematite.

Modelling of the preventive PAA effect on iron

The objective of this modelling work was to show that iron quantity increases at SG blowdown when PAA is injected to a sufficient level in the SG circuit. It would confirm the preventive effect of PAA on iron. The chemical code PhreeqCEA-3.2 version dedicated to reactors application was used. This code, combined with thermohydraulic data from literature, also allowed us to estimate the blockage of the last Tube Support Plates (TSPs) and the steam composition.

In order to integrate the PAA effect on the SG fouling, the experimental results of Test 0.1 (C_{PAA} = 0.1 mg.kg^{-1}) about the complexing/dispersing effect of PAA on iron oxides (D'ANGELO, 2015; ROY, BLANCHARD, et al., 2014) were integrated in the chemical code. Indeed, the mean quantity of iron measured at the liquid output is equal to 13 µg.kg^{-1}. A first assumption was that several carboxylic groups are needed to complex iron (II). The species containing the carboxylic groups needed to complex iron (II) is a ligand, L with an oxidation number –II. We have supposed that the PAA mass concentration is proportional to the one of the ligand L, 13 µg.kg^{-1} (*i.e.* 0.1804×10^{-6} mol.kg^{-1}) of L are needed to complex all the iron present in solution.

The simulation was performed on a SG of Pressurized Water Reactor (PWR). A recirculation of the solution overall the SG is considered. The presence of a blowdown circuit[2] and singularities such as tube support plates were also considered. Three phases are present in the SG: the Inconel tube (solid), the steam and the liquid.

Figure 8 represents the chosen mesh (29 control volumes) that can be described as follows:
- ten control volumes for the spillway;
- one control volume for each TSP;
- one control volume between two TSPs;
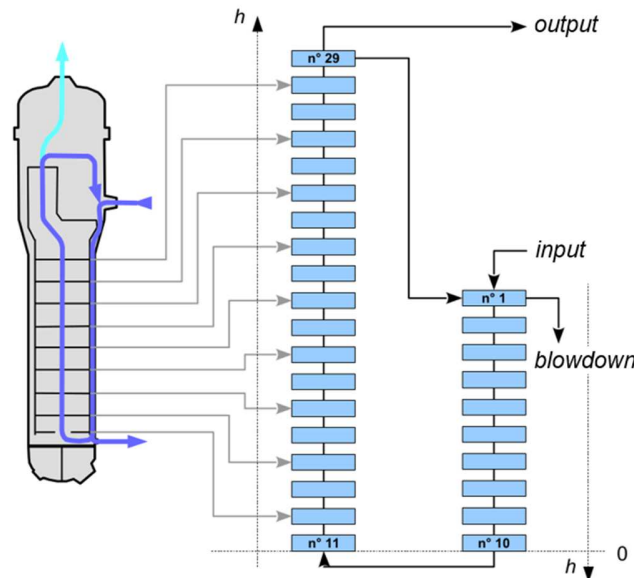- one control volume before the first TSP and one after the last TSP.

Figure 8. SG mesh, h is the height in the SG. Each blue square is a control volume (YOU, 2016)

A thermohydraulic dataset (temperature and water steam weight in particular) was constructed from thermohydraulic data of a 1300 MW PWR given by (GIRARD, 2012). For the other physical conditions, the input data were the following:
- mass flow at the entrance of SG, 1932 t.h^{-1} for one SG;
- tubes number, 5342;
- blowdown ratio, 0.01 *i.e.* 1 % of the feedwater flow;
- temperature of the feedwater at the SG entrance, 250 °C.

The chosen chemical composition of the SG feedwater is summarized in Table 3.

---

[2] In this version 0 of the chemical code, the blowdown is not well situated for mathematical simplification

Table 3. Chemical composition of the SG feedwater used for the calculations

[NH$_4$OH]	[H$_2$]	[Fe]
(mol.kg^{-1})	(cm$^3_{TPN}$.kg^{-1})	(mol.kg^{-1})
234×10^{-6}	5	26.8×10^{-9}

The results of the calculations give all the species quantities in the solution and also the amount of precipitated magnetite. The quantities are given as surface density in order to be comparable.

The calculated iron quantity at blowdown without addition of ligand is $2.94×10^{-8}$ mol.kg^{-1} (≈ 1.6 µg.kg^{-1}). When 13 µg.kg^{-1} of ligand L are injected in the SG, the iron content reaches $3.278×10^{-8}$ mol.kg^{-1} (≈ 1.8 µg.kg^{-1}). As a consequence, a 11.5 % increase of total iron quantity (*i.e.* iron (II) and (III)) at blowdown was determined.

Moreover, the deposition of magnetite has significantly decreased when PAA has been injected. The quantity of magnetite is given as apparent magnetite thickness on a SG tube (see Figure 9). The addition of PAA in the SG leads to a decrease of magnetite thickness of one order of magnitude. The calculations show no precipitation of hematite.

The estimated magnetite thickness on a SG tube without PAA is 40 µm after one year of nominal operating conditions. An addition of 13 µg.kg^{-1} of ligand leads to a total absence of deposit at the 5th TSP level.
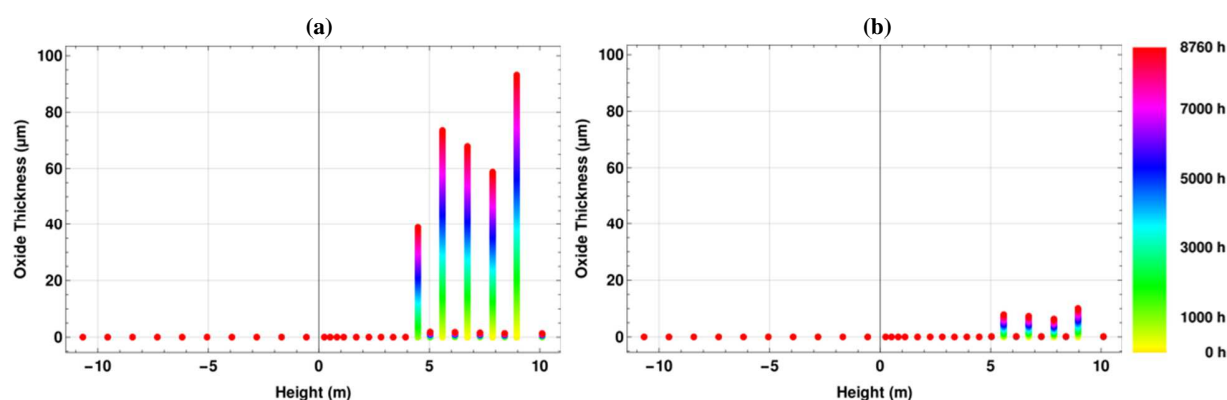

Figure 9. Apparent thickness of iron oxide on a SG tube as a function of the height in the SG (a) without PAA and (b) with 13 µg.kg^{-1} of ligand. Operating time ranges between 0 and 8760 h (see the legend) *i.e.* one year of nominal operating conditions

CONCLUSION

The aim of this study was to evaluate the preventive nature of PAA on the fouling deposits (mainly composed of iron oxides) in SGs and to determine the action mechanism(s) of PAA on iron oxides.

In order to determine the effect of PAA on the formation of magnetite deposits, Inconel 690TT tubes were exposed to the secondary chemistry medium and magnetite particles with and without PAA.

The main conclusions are firstly that the dissolved iron content is increased by a 3.3 factor on average at the liquid exit in the presence of PAA and can be up to 6 times higher than the iron content measured

without PAA. As a consequence, the effectiveness of PAA was shown for a concentration of 0.1 mg.kg^{-1} in the liquid phase of the autoclave, equivalent to 0.001 mg.kg^{-1} in the SG feedwater.

Secondly, a decrease in the oxide deposit (magnetite) formed on the surface of the tube in the presence of PAA was observed by scanning electron microscopy and confirmed by XRD analysis.

Moreover, the presence of PAA in the circuit leads to the formation of hematite (α-Fe$_2$O$_3$) on the tube surface of Inconel 690TT. The formation of hematite seems to be due to the complexation of iron (II) by PAA. This complexation leads to the increase of iron (III) in solution that precipitates as hematite which could have been deposited on the surface.

The modelling work was performed with the chemical code PhreeqCEA-3.2 version combined with thermodynamic data from the literature. The results of the simulation performed on a SG of Pressurized Water Reactor (PWR) including an injection of PAA confirmed the preventive effect of PAA on iron oxide. Indeed, a 11.5 % increase of total iron at blowdown was estimated for a ligand injection of 13 µg.kg^{-1}. The calculations also showed a decrease of magnetite thickness of one order of magnitude when a small amount of PAA is injected.

NOMENCLATURE

CEA	Atomic Energy Center
IRIS	CEA loop: Research Instrumentation for the Investigation of Speciation in aqueous media at high temperature
[M]	Mass concentration or molality of the molecule M, measurement unit is specified
NPP	Nuclear Power Plant
P	Pressure (Pa)
PAA	Polyacrylic acid
PWR	Pressurized Water Reactor
$S_{Fe}(T)$	Iron solubility at the temperature T
SG	Steam Generator
T	Temperature (°C)
t_R	Retention time (h)

REFERENCES

Angwin, M. J. (1986). *Use of Pourbaix Diagrams to Infer Local Pitting Conditions* (No. NP-4831). EPRI.

D'Angelo, R. (2015). The effects of dispersants on the fouling and the blockage deposits in pressurized water reactor steam generators. Université Pierre et Marie Curie.

EPRI. (2002). *Dispersants for Tube Fouling Control - Volume 3: Qualification for a Long-Term Trial in a Replacement Steam Generator Tubed with Alloy 690 TT* (No. 1002774). EPRI, Palo Alto CA.

EPRI. (2012). *Dispersants for Pressurized Water Reactor Secondary Side Fouling Control: Sourcebook for Online and Offline Applications: Volume 1 & 2* (No. 1025317). EPRI, Palo Alto CA.

Girard, S. (2012). *Diagnostic du colmatage des générateurs de vapeur à l'aide de modèles physiques et statistiques*. École nationale supérieure des mines de Paris.

Laire, C., Ceursters, D., S., B., Delporte, R., Coart, S., & Lecocq, R. (2014). First Steam Generator Cleanup Application with Dispersant at Doel 3. *Nuclear Plant Chemistry Conference, Sapporo, Japan*.

Pourbaix, M. (1963). *Atlas d'équilibres électrochimiques, publisher = Publication du centre Belge d'étude de la corrosion*. (CEBELCOR, Ed.) (Vol. 660–15, p. 645). Gauthier-Villars.

Reiller, P., Janiaux, N., Colette, S., Mertens, V., You, D., & Plancque, G. (2011). *Colmatage des générateurs de vapeur : études bibliographique et expérimentale de l'effet dispersant et/ou complexant de l'acide polyacrylique* (No. 11-045 indice B). CEA.

Roy, M., Blanchard, E., Mertens, V., & You, D. (2014). *Effet préventif de l'acide polyacrylique contenu dans l'Optisperse PWR-6610 sur l'encrassement d'un tube d'alliage 690.* (No. DPC/SECR/NT/2014/023 Indice A). CEA Saclay.

Roy, M., Mansour, C., & You, D. (2014). The Effect of Polyacrylic Acid on Iron Oxides Formed on Steam Generator Tubes and on Metallic Copper Present in Pressurized Water Reactors. *Nuclear Plant Chemistry Conference, Sapporo, Japan.*

Sapieszko, R. S., & Matijević, E. (1980). Preparation of well-defined colloidal particles by thermal decomposition of metal chelates. I. Iron oxides. *Journal of Colloid and Interface Science*, *74*(2), 405–422. doi:10.1016/0021-9797(80)90210-6

You, D. (2016). *Installation et utilisation de l'IHM-Colma. Colmatage de GV* (No. DPC/SECR/ST/2016-014). *CEA - I3P*. CEA.